Dielectric Spectroscopy: Revealing the True Colors of Biological Matter

Marie Mertens, Maede Chavoshi, Olivia Peytral-Rieu, Katia Grenier, Dominique Schreurs

Dielectric Spectroscopy: Revealing the True Colors of Biological Matter

Marie Mertens[1], Maede Chavoshi[2], Olivia Peytral-Rieu[3], Katia Grenier[3], and Dominique Schreurs[2]

[1]KU Leuven, 3001 Leuven, Belgium and Polytechnique Montréal, Montreal, QC H3T 1J4, Canada.

[2]KU Leuven, 3001 Leuven, Belgium.

[3]LAAS-CNRS, Université de Toulouse, CNRS, UPS, 31400 Toulouse.

1. Introduction

Accurate characterization of biological matter, for example, in tissue, cells, and biological fluids, is of high importance. For example, early and correct detection of abnormalities, such as cancer, is essential as it enables early and effective type-specific treatment, which is crucial for mortality reduction [1]. Moreover, it is imperative to investigate the effectiveness and toxicity of pharmaceutical treatments before administration in clinical practice [2]. However, biological matter characterization still faces many challenges. State-of-the-art imaging and characterization methods have drawbacks, such as the requirement to attach difficult-to-find and costly labels to the biological target (e.g., COVID-19 rapid test), expensive equipment (e.g., magnetic resonance imaging or MRI), low accuracy (e.g., ultrasound), use of ionizing radiation (e.g., X-rays), and invasiveness [3]. The characterization of biological matter using microwave (μW), millimeter wave (mmW), and Terahertz (THz) spectroscopy is a promising

alternative: it is label-free, does not require ionizing radiation, and can be non-invasive. Moreover, there is a significant difference in how different biological materials absorb, reflect, and transmit electromagnetic (EM) waves [4] that is due to the difference in their dielectric properties. The dielectric properties are described by the frequency-dependent material parameter called the complex permittivity $\boldsymbol{\varepsilon(f)}$, which expresses how the material responds to an external oscillating electric field. The complex permittivity of a material determines how the material absorbs, reflects, and transmits EM waves at different frequencies (Fig 1.). Since each biological material's permittivity spectrum is different, it acts as an electromagnetic fingerprint. A material's complex permittivity can be calculated from the reflection and transmission of electromagnetic waves through the material, described by the scattering (S)-parameters, which can be measured using a Vector Network Analyzer (VNA) transmitting and receiving EM waves over a range of frequencies. The amplitude and phase of the transmitted and reflected EM waves at different frequencies are influenced by different underlying biological effects at different scales. That causes the entire spectrum to provide information from the supracellular to the molecular and even atomic scale.

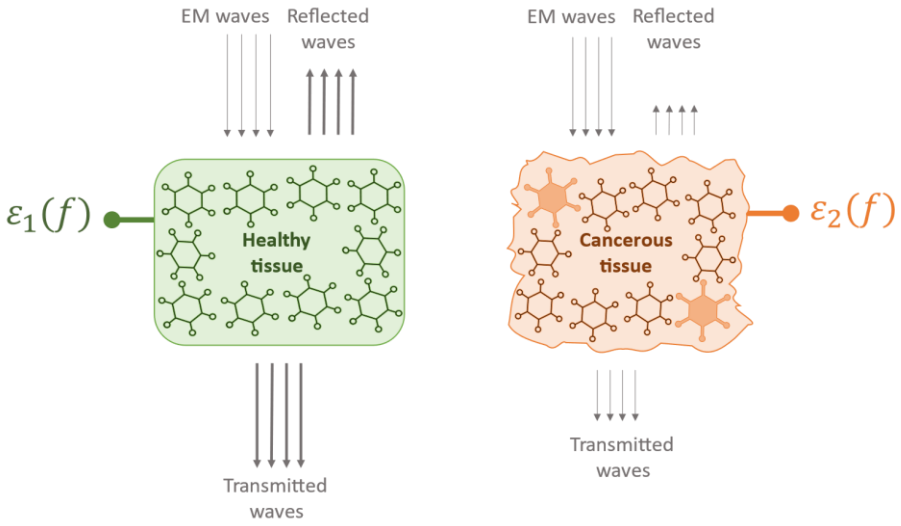

Figure 1. Conceptual illustration of how biological tissues (e.g., healthy and cancerous tissue) absorb, reflect, and transmit EM waves differently caused by the difference in their dielectric spectra.

Spectroscopy using µW, mmW, and THz EM waves has shown potential to sense the concentration of important biomarkers, such as glucose in diabetes patients, DNA and proteins that inform about genetic disorders, and cancer biomarkers to distinguish healthy matter from cancerous matter [4]. These applications will be further elaborated on in a later section on Dielectric Spectroscopy Techniques.

2. Dielectric Spectrum

In this section we explain the meaning and interpretation of the dielectric spectrum, representing complex dielectric permittivity as a function of frequency. The physical phenomena underlying the spectrum's most important features are elaborated on in the subsections on relaxations and resonances.

2.1 Dielectric permittivity

As opposed to most non-biological materials, the dielectric permittivity depends heavily on the frequency of the applied electric field for biological matter. Indeed, at different frequencies, the material will absorb, reflect, and transmit EM waves differently. Moreover, permittivity is a complex material parameter:

$$\varepsilon(f) = \varepsilon'(f) - j\varepsilon''(f) \quad (1)$$

A schematic representation of both the real and imaginary parts of the dielectric permittivity is shown in Figure 2. The real part of permittivity describes how well the electric dipole

moments inside the material align to the electric field. The imaginary part of the permittivity describes the EM losses into the surrounding media. These EM losses can be considered to originate in the friction caused by the movement of the charges aligning to the electric field. More fundamentally, the permittivity describes polarization, and the magnitude and phase describe its extent and delay, respectively. The dielectric spectrum shows relaxation and resonance phenomena. Figures 3 and 4 illustrate the relaxation and resonance phenomena. At the frequency of the relaxation phenomena, also called dispersion, there is a decrease in the real part of permittivity, whereas at the frequency of the resonance phenomena, a sharp resonance is seen in the real part of the permittivity. These phenomena will be further explained in the following section.

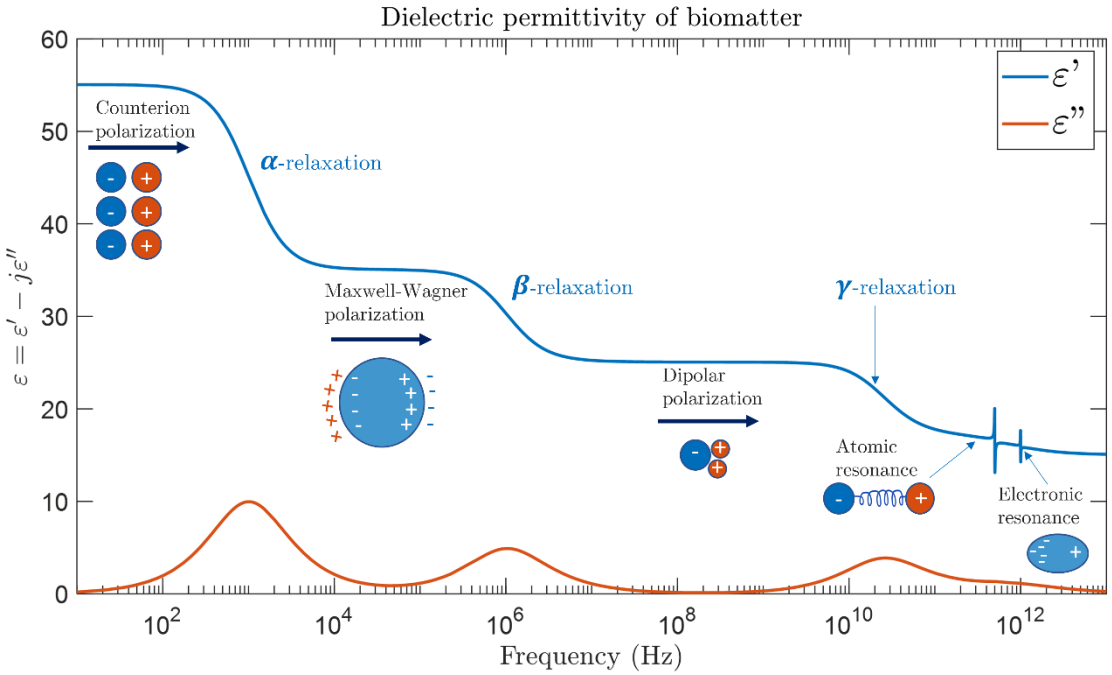

Figure 2. Complex permittivity of biomatter. Similarly represented in [4].

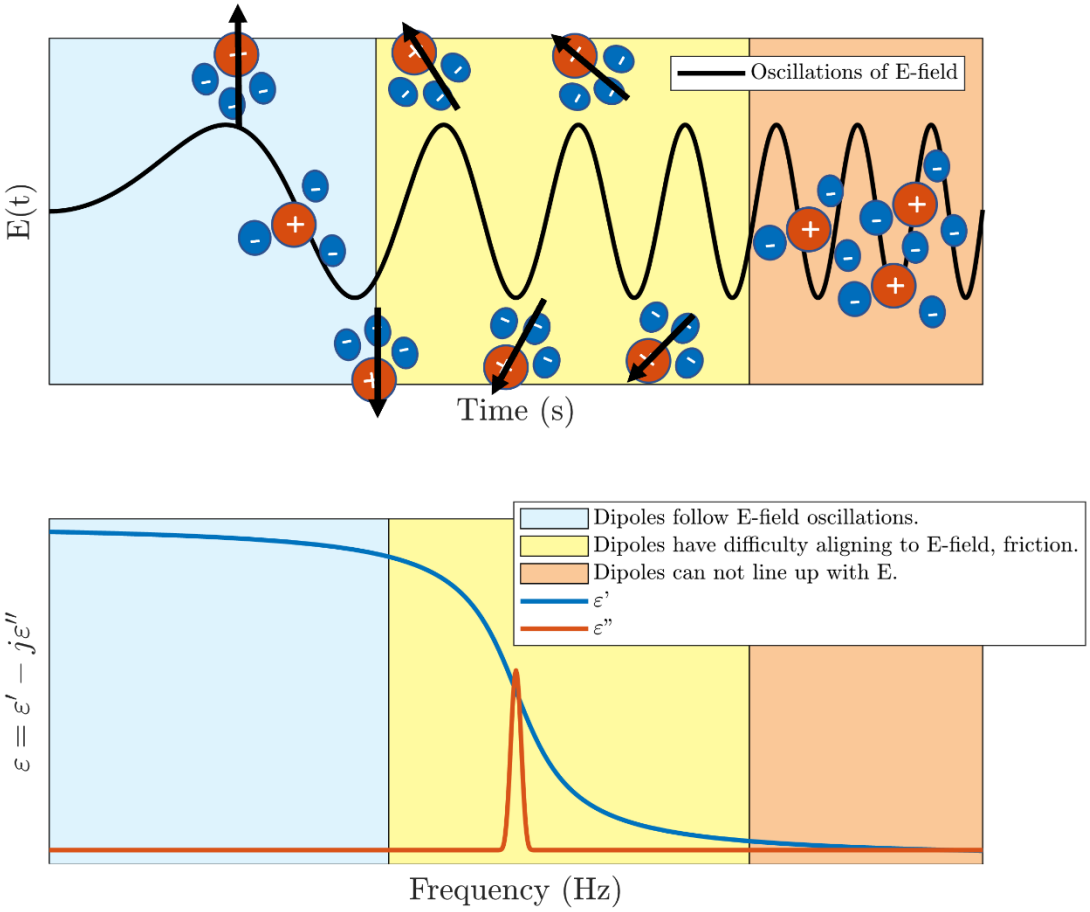

Figure 3. Conceptual illustration of dispersions in permittivity spectrum: as the frequency of the electric field oscillations rises, dipole moments start to be unable to align to the electric field and their contribution to permittivity lowers, seen in a decrease in the real part of permittivity.

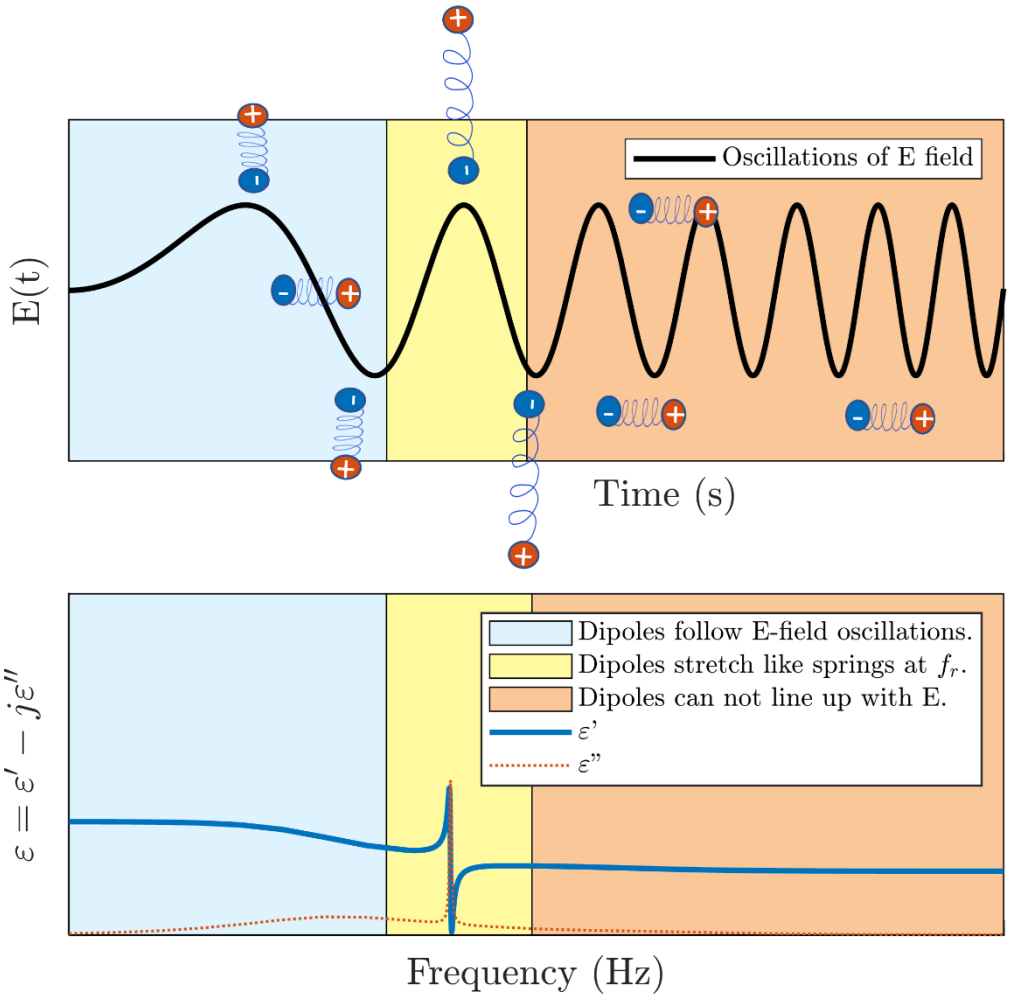

Figure 4. Conceptual illustration of resonances in permittivity spectrum: as the frequency of the electric field oscillations reaches the dipole's resonance frequency, its bound charges resonate to the electric field, stretching out and aligning to it with maximal polarization as they are being pulled apart the furthest.

2.2 Permittivity relaxations

An intuitive explanation for the relaxations (or dispersions) in the real part of the permittivity is given here: an external oscillating electric field causes the alignment of dipole moments (due to the motion of ions, atoms, and molecules) inside the material to the electric field. The

larger this alignment, the larger the total electric field and the larger the real part of the permittivity. When the charges' inertia causes their inability to follow the electric field's oscillations, their contribution to the total electric field drops to zero. This can be seen in the spectrum as a drop in the real part of the permittivity and is called a relaxation [3], which is visualized in Figure 3. At each dispersion, there is a peak in the dielectric losses, which can be seen in the imaginary part of the permittivity. This frequency range is indeed where the charges are most out of phase, delayed to the external electric field, causing the presence of an imaginary component in the polarization. The relaxation event does not occur at one single frequency but over a range, as biological matter is highly heterogeneous and the different ions, atoms, and molecules have slightly different relaxation frequencies. The various relaxation mechanisms (α-, β- and γ-dispersion) are determined by distinct polarization mechanisms for the different constituents of matter (cells and cell membranes, ions, molecules, atoms, electrons) [5]. As such, the spectrum informs us about the different constituents of matter in different frequency bands. It is essential to understand the fundamentals behind the relaxation phenomena to understand how one could extract information on the biological and physiological state of a material from the frequency spectrum.

2.2.1 α-dispersion

The first relaxation is called α-dispersion. It is caused by the inability of ions to respond to a fast-changing field, and occurs at Hz to kHz frequencies. Unfortunately, due to high measurement uncertainty through unwanted measurement electrode polarization, α-dispersion can often not be interpreted accurately in terms of permittivity [6].

2.2.2 β-dispersion

The second relaxation is called β-dispersion. It is caused by the disappearance of Maxwell-Wagner polarization at the frequency of the dispersion at kHz to MHz frequencies. This Maxwell-Wagner polarization is caused by the presence of physical interfaces (e.g., cell membranes) that constitute the border between two different media, such as the intracellular and the extracellular fluid. At frequencies lower than the β-dispersion, and upon the effect of an external electric field, charges accumulate at the border and create a space charge region, which contributes to the permittivity. At frequencies higher than the β-relaxation, these interfaces are shortened, and they become invisible to the electric field, which can now penetrate to the insides of the cell [4], [6], see Figure 5. As such, when investigating permittivity at frequencies beyond the β-relaxation, examination of the cells' contents (e.g., intracellular fluid and particles) becomes possible. Because of the disappearance of the space charge region, there is a decrease in polarization and as such a decrease in permittivity.

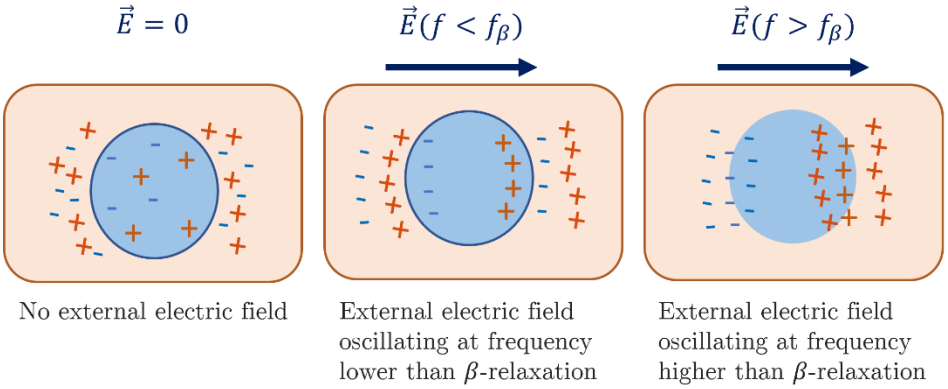

Figure 5. An illustration of the concept of β-relaxation, where the Maxwell-Wagner polarization disappears because the electric field oscillations bypass the cell membranes at frequencies beyond the β-relaxation.

2.2.3 γ-dispersion

Finally, γ-dispersion occurs at frequencies near 24 GHz. This dispersion is highly influenced by the water content of the material, which is often high for biological matter. At frequencies below the γ-dispersion, the dipole constituted by the asymmetric shape of a free water molecule vastly contributes to the induced polarization when it aligns to the external electric field. However, around 24 GHz, these molecules are unable to align with the external electric field [4], [6]. The higher the free water content, the higher the orientation polarization and the higher the permittivity before the γ-relaxation. Given that water content varies between different organs, tissues and cells, measuring permittivity around the γ-relaxation can help in differentiating between different organs for microwave imaging, between live and dead cells, or between cancerous and healthy cells, and so forth. A separate dispersion is attributed to water molecules that are bound to other molecules. Given the complexity of this δ-dispersion, it will not be elaborated on here.

2.3 Permittivity resonances

The physical events underlying the resonances in the THz part of the spectrum are rather complicated. However, we will attempt to describe the fundamental idea: when the external electric field is oscillating at THz frequencies (1 000 000 000 000 oscillations per second!), only few very small biological structures are still able to align to the electric field and can as such contribute to the polarization. These small structures are (1) the electrons in the electron cloud surrounding their positive core, and (2), atoms that are attached to each other in a molecule. The electric field not only rotates them but also pulls apart the positive and the negative parts, after which a restoring force acts to bring them back together; the structures then can be considered as if they were springs [2]. At their resonance frequency, the distance

between the positive and the negative parts reaches its maximum, first in the direction of the external electric field (local permittivity maximum), then, because of delay to the electric field, in the opposite direction (lower the total electric field, local permittivity minimum). This is illustrated in Figure 4. There is a peak in losses because of the energy absorption that comes with the separation of the charges. Changes in the concentration of some important biomolecules can be observed as a shift in resonant frequency in the dielectric spectrum as their vibrational frequency lies in the frequency range of 300 GHz to 1 THz [4].

To conclude, the α-, β-, and γ- dispersions and the electronic and atomic resonances that appear in biological matter's frequency spectrum are influenced by different biological events. Researchers can measure the whole frequency spectrum and deduct information about all these biological events at the same time. Indeed, researchers can characterize biological matter based on fundamental characteristics of the spectra, such as how broad each dispersion is, and at which frequency each relaxation occurs. Examples of how scientific research used these characteristics for biological matter characterization are given in the following section. However, in practice, not many have succeeded to really link these parameters to specific biological events and so the field still needs to advance in this area. Moreover, the frequency of characterization can be chosen according to which biological events are of interest to the research (*e.g.,* β-frequencies to obtain information on number of cells and cell membranes, and γ-frequencies when water content is of interest).

Finally, before diving into the practical aspects of permittivity measurements, we ought to clarify one thing: one might wonder why we choose to consider dielectric constant rather than impedance. Some [7] prefer to consider impedances which, as opposed to dielectric permittivity, are directly measurable, and no difficult mathematical transformations or

calculations are required to obtain them. For the characterization of two or more cells, which always comprise the same geometry and are measured with the exact same method, one is completely right to consider impedances. However, as “dielectric electrical (oxymoron) engineers” [7], we consider dielectric permittivity to be the fundamental parameter. It is a material characteristic and should as such, after de-embedding, be independent of the measurement method and size and shape of the MUT, which is not true for impedances. Even though still to be improved in practice, the dielectric permittivity of cells, tissues and liquids of different sizes should thus reflect only the content of the biological matter rather than the size, shape and volume of the cell.

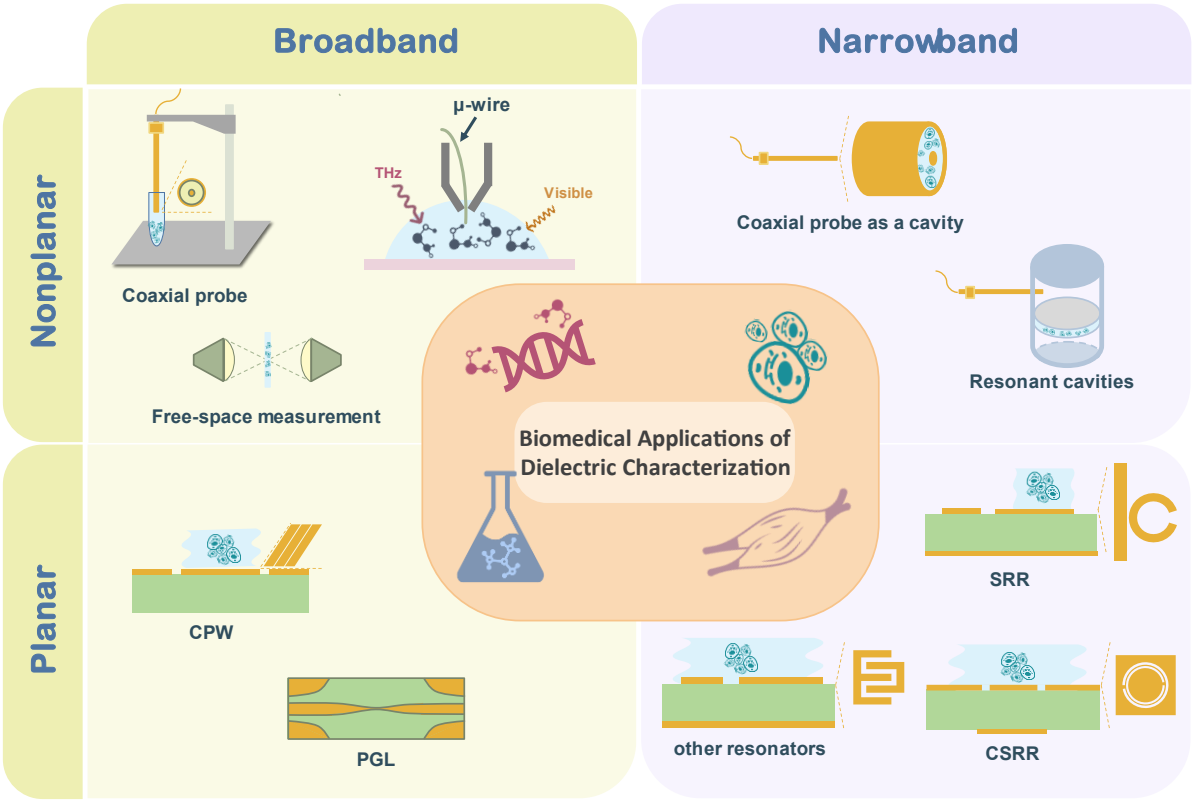

Figure 6. Illustration of different types of microwave sensors for dielectric characterization of biological matter.

Table 1: Overview of dielectric characterization methods for biological matter and their applications.

Dielectric characterization methods		
Method	**Broadband/narrowband Planar/Non-planar Frequency Range**	**Example applications**
Coaxial Probe	Broadband, non-planar 10 MHz-110 GHz	Mainly tissue characterization: e.g., breast tissue [10], liver tissue [11], renal calculi [12]
Coplanar Waveguide	Broadband, planar < 1 GHz – sub-THz	integration with microfluidics for measurements of small volumes: e.g., single cell detection and analysis [21],[22], detection of mitochondrial activity [26] detection of skin melanoma [27]
Microwire	Broadband, non-planar Sub-THz	Detection of protein resonances [33], [34]
Planar Goubeau Lines	Broadband, planar Sub-THz-THz frequencies	Lysosome dielectric spectroscopy [35]
Free-space measurements	Broadband, non-planar 50 GHz-THz	Upcoming technology for FDS
Cavity resonator	Narrowband, non-planar	Water-based solutions such as NaCl [37]
Planar resonators: SRR, CSRR, …	Narrowband, planar	Bacteria [44], [45], [46], [47], [48], glucose [51], [52], [53], [54], [55], colon tissue [50], [56], skin tissue [57], cells [39], [40]

3. Dielectric spectroscopy techniques

Dielectric spectroscopy (DS) is the measurement of the material's fundamental dielectric properties as a function of frequency. These properties can be interpreted as explained above and employed to characterize biological matter. The general methodology consists of (1) the measurement of the reflection and/or transmission of EM waves as S-parameters through the material under test (MUT), followed by (2), a mathematical conversion to dielectric permittivity. The former will be discussed below. The latter depends on the geometrical setup of the measurements, as well as the size and the shape of the MUT and the calibration method, and will not be explained in detail further in this article. The basic principle is that the measurement results will be de-embedded i.e., the effects of the setup will be removed, until only the effect of the MUT's permittivity is visible. Alternatively, an analytical description of the effect of the sample's permittivity in the measurement results can be employed, from which the permittivity can directly be extracted.

The most common methodologies for measurement of S-parameters of biological matter for reflection and transmission are explained below and illustrated in Figure 6 and Table 1. Some applications are given as well, and it is shown how the methods have been selected and adapted for measurements on biological matter. For example, biocompatibility of the measurement device must be guaranteed and possible EM-heating effects must be prevented. The preferred method depends on the frequency, the physical and chemical attributes of the biological MUT (liquid/solid, size, etc.), and the requirements in terms of sensitivity and limit of detection among others. Moreover, the operating bandwidth of the measurements plays a key role in selecting the technology. Broadband characterization provides a global measure on a broad range of frequencies, and thus lets us know about the

constituents of the matter on different scales, but requires technology that is appropriate for the whole spectrum. The technology can be hard to develop, and the instrumentation can be costly and fragile. Narrowband characterization, on the other hand, focuses on one to a few discrete frequencies so that the device can be designed to be optimized to these frequencies using cheaper and simpler components. These measurements are often more precise and easier to develop. Below we will first elaborate on broadband dielectric spectroscopy (DS), and then the main approaches and applications for narrowband characterization will be explained.

3.1 Broadband Dielectric Spectroscopy

In this subsection the most common approaches for broadband dielectric spectroscopy of biological matter are discussed. More specifically, coaxial probes and coplanar waveguides are first explained in depth, after which we summarize the upcoming technologies for sub-THz and THz broadband characterization.

3.1.1 Open-ended coaxial probe

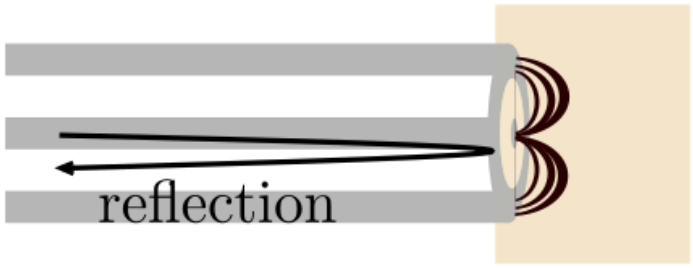

Figure 7. Open-ended coaxial probe method.

An open-ended coaxial probe is commonly used for measurements of the reflection of EM waves (S_{11}) from a biological MUT in the frequency range from $\pm 0.1 - 10$ GHz (and sometimes even for measurements up to 110 GHz). As the coaxial transmission line is cut off at the border with the MUT, its field fringes into the liquid or semi-solid biological matter, which affects the reflection of the EM waves [8]. The basic concept is illustrated in Figure 7. The conversion method from reflection to permittivity is well established, and the method requires minimal sample preparation and is easy to use [9]. The coaxial probe has mainly been used to characterize biological tissue, from normal, benign, and malignant breast or liver tissue to renal calculi and muscle [10], [11], [12]. The measurement methodology had to be adapted largely for biological tissue when researchers noticed that the practices were not proper for biological matter. Indeed, it was found necessary to control the precise position

and pressure of the probe on the tissue, as compressing the semi-solid would change its dielectric properties [6]. Moreover, in a large-scale breast tissue investigation performed by Lazebnik et al. [10], it became clear that an analysis of the content of excised tissue before measurement was of critical importance. A large difference was found between dielectric properties of normal breast tissue and malignant tissue, but it appeared to be largely determined by the adipose (fatty) content of the tissue sample, which was higher in the excised healthy samples. The differences between healthy and malignant tissue were far smaller when this adipose content was accounted for [10]. Nevertheless, other studies still showed promising results: O'Rourke et al. [11] showed that the dielectric properties of ex vivo malignant liver tissues are 19 to 30% higher than normal tissue. Moreover, the renal calculi (kidney stone) category can be statistically differentiated by dielectric properties over the frequency range from 500 MHz to 18 GHz [12].

3.1.2 Planar transmission lines

Transition from non-planar setups to planar ones enables measurements on smaller samples and as such is interesting for the measurement of extracted biological liquid and tissue samples, and cell suspensions. Dielectric matter characterization can be performed using many types of transmission lines, such as coplanar waveguides (CPW), microstrip lines (ML), substrate integrated waveguides (SIW), and planar Goubau lines (PGL) for higher frequencies. However, most of these methods, as for example ML and SIW, are mainly used for characterization of the dielectric substrate that they are fabricated on, as their modes of propagation show maximum electric field distributions in the substrate (often between a metallic ground plane and the transmission line). They thus rely on the deposition of metallic lines *onto* the MUT. Characterization using CPW (or PGL, see next section) can be performed by putting the sample – contained in a biocaptor- on top of, and thus directly in contact with

the metallic lines that are deposited onto another low-loss dielectric material. Gold is often used for these metallic lines as it allows for maximum biocompatibility, resistance against oxidation when measuring ionic substances, and a good transmission of the EM waves.

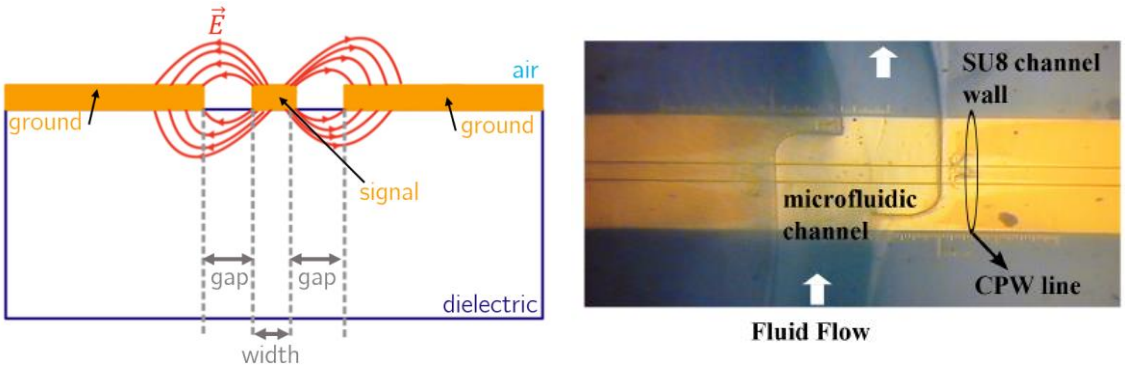

(a) (b)

Figure 8. (a) Propagation of electric field in quasi-TEM mode. (b) microfluidic channel on top of CPW line for liquid characterization [13].

In CPW the electric field lines in the dominant mode of propagation, quasi-TEM mode, are oriented as shown in Figure 8 (a) [14]. The propagation of the electric field will be affected by any biological matter put on top of the transmission lines. The effective permittivity of the CPW lines is a mathematically complex combination of the permittivity of the dielectric and the permittivity of the material on top of the lines (the unknown editor of Microwaves101 [15] provides us with the rule of thumb that it is approximately the average). In most devices, a microfluidic channel, sometimes with hydrodynamic traps, functions as biocaptor and is constructed on top of the CPW lines (Figure 8 (b))- mainly on the signal line and gaps where the field is largest - to allow the electric field to be affected by the biological matter that is pumped through the channel [16],[17]. In fact, as the position of the biological object (e.g., cell, organelle) must be controlled to maximize the sensitivity, “trapping” structures can be

added to the microfluidic structure [18], [19]. As CPW operates in the GHz frequency range, where the electric field can probe the inside of the cells through the shortening of the capacitive effect of the cell membrane, it is used extensively in investigating the intracellular components of different cell lines and their reaction to chemical and physical treatment [18], [20], [21], [22]. Moreover, CPW lines can be adapted to measure the dielectric properties of biological matter of different sizes: from in-vivo tissue characterization down to single cells, making it a promising technique to monitor the effects of drugs on different biological entities in a label free, non-invasive, and non-destructive way [16], [17]. Different studies have shown the possibility to monitor cell electroporation, electrochemotherapy, and the effect of saponin and mitochondrial activity at single cell or cells in suspension level as represented respectively in the first and second images of Figure 9 [23], [24], [25], [26]. For instance, in [23], it was found that saponin, which affects the cell membrane and allows for exchange of contents through the membrane, effectively caused a reduction in dielectric contrast between the extracellular and intracellular medium. Furthermore, mitochondrial activity can be monitored. This is important as it can be an indicator for how cells will react to therapy. Moreover, melanomas (skin cancers) have been studied directly in vivo and can be detected using microwave spectroscopy with a sensor in contact with the skin of the subject, as represented in the fourth image of Figure 9 [27]. Finally, the dielectric characterization of microtissue (*3D cell aggregates as a model for cancer tissue*) is emerging with the device represented in the middle of Figure 9 [19], [28]. In conclusion, CPW allows studies in multiple bio-sample scales as summarized in Figure 9. [19],[23], [27],[28],[29].

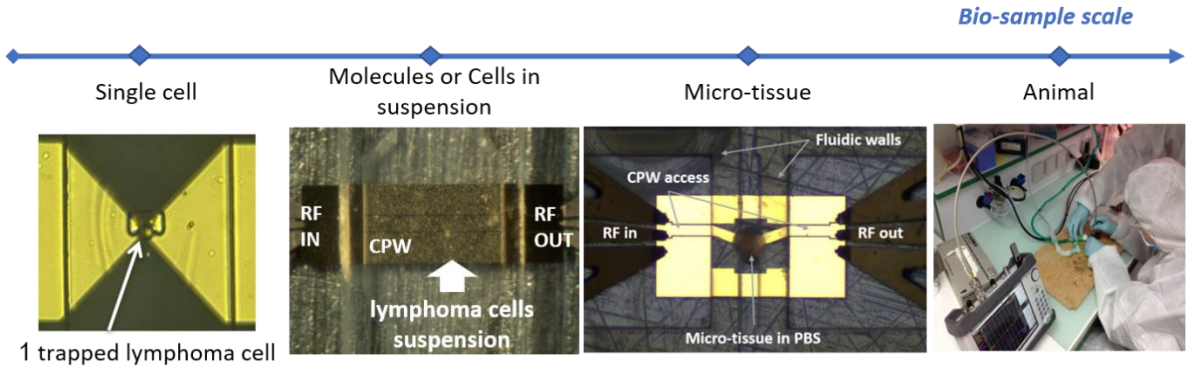

Figure 9. Examples of microwave transmission-based sensors depending on bio-sample scale for dielectric characterization showing the versatility of CPW sensors in biological applications [19],[23], [27],[28],[29].

3.1.3 Sub-THz and THz measurements

In this paragraph, we list interesting technologies for broadband sub-THz and THz measurements (0.1 THz – 10 THz). These frequency ranges show great potential for dielectric characterization. THz Time Domain Spectroscopy (TDS) has been shown to be able to detect drug effectiveness through comparison of absorption coefficients and refractive indices in [30]. It was found that these coefficients and indices showed the trend towards healthy tissue when a drug was administered and the negative effect on the healthy cells, respectively. Moreover, in [31] promising results were obtained showing significant differences in the THz absorption spectrum for different histological types, pathological grades, and glioma-specific biomarkers in measurements of healthy and cancerous brain tissue. In [32] myocardial amyloidosis (deposition of specific protein causing heart stiffness) was detected using THz-TDS, combined with convolutional neural networks. Finally, as mentioned in the explanation of dielectric permittivity, the frequency spectrum overlaps with the resonance frequencies of important proteins and biomolecules in this range. To extend these methods for a more

accurate frequency domain analysis with higher frequency resolution, there is a need to establish Frequency Domain Spectroscopy (FDS) methods at THz frequencies. Technologies are being developed to cope with the high loss of EM power into lossy biological MUT and the high noise that is inherent to these frequency bands. For instance, [33] showed the use of a microwire to detect resonating proteins at 0.314 THz excited by visible light. Moreover, a protein concentration change effectively caused a change in the measured resonance frequency in [34]. Planar alternatives are being researched as well, such as the Planar Goubau line (PGL), a fine microstrip line with no ground onto which the Goubau mode can be excited through CPW to PGL transition. This mode shows high confinement around the line and can be used for measurement of extremely small structures close to the line. In [35] transmission through lysozymes was successfully measured using PGL. More research is necessary to investigate the further capabilities of PGL. Finally, research is ongoing for the use of Free Space Measurements (FSM) of biological cells and tissues. Interestingly, the sub-THz to THz measurements are hovering on the border between THz spectroscopy and visible light spectroscopy, slightly further from our field of knowledge, but definitely not less important. Researchers are exploring the borders of both the microwave and light (towards quantum) theories and verifying how it can be crossed.

3.2 Narrowband Characterization of Biological Matter

The technologies and applications discussed so far are mainly used for broadband dielectric spectroscopy of biological matter, i.e., in a wide frequency range. However, broadband permittivity information is not necessarily needed in many cases; for example, if one is interested in studying the presence or absence of a specific substance, solution

concentrations, and viability and growth of cells or organisms like bacteria, among others, at a single frequency or in a small frequency range, narrowband techniques can be more precise and faster to investigate dielectric properties of materials.

Narrowband measurements often employ a resonance-based microwave sensor that concentrates the electric field at frequencies near a specific frequency, depending on the application. The term “resonance” in this section is different than the one used in the prior sections; here, we mean the resonance of a circuit, due to its components. Depending on the structure of a sensor, it can be modelled as a resonant circuit, including an inductance *L*, capacitance *C*, and a term relating to conductivity (or inversely, resistance) *G* or *R.* Depending on modelling, they can be connected in a series or parallel form.

This is how these resonant sensors come into play: the sensor behaves as a series or a parallel RLC circuit with its components tuned by the MUT’s properties. For instance, the resonance frequency f_{res} and the quality factor Q define the resonance behavior of the sensor. Although the precise relation depends on sensor configuration and calibration, we can approximately assume that the resonance frequency (determined by the equivalent inductance *L* and capacitance *C*) is related to the permittivity as

$$f_{res} = \frac{1}{2\pi\sqrt{LC}} \propto \frac{1}{\varepsilon}$$

(2)

and the quality factor can be inversely related to the losses as

$$Q \propto \frac{1}{\tan\delta}$$

(3)

Thus, the interaction of the highly concentrated field and the MUT determines the system's frequency response by changing

$$f_{res_0} \rightarrow f_{res_1}, and\ Q_0 \rightarrow Q_1 \tag{4}$$

(4)

Nevertheless, challenges in resonance-based biological matter measurements arise from the fact that a considerable portion of them consists of a highly lossy substance: water! The loss decreases the quality factor, flattening the resonance dip and making it difficult to find the resonance frequency.

Various types of planar and non-planar microwave resonant sensors are used for dielectric spectroscopy of different biological matter, ranging from aqueous biological solutions, like glucose or saline solutions, to cells and tissues. Here, we subdivide the narrowband technologies into non-planar cavity resonators and planar resonators.

3.2.1 Non-planar Cavity Resonators

In the case of non-planar cavity resonators, devices such as coaxial resonators have been developed to study the concentration of solutions. As the name implies, a cavity consists of a hollow space filled with the sample, and the resonance behavior changes according to the sample's permittivity.

As discussed previously, in wideband open-ended coaxial probe measurements, the sample is in contact with the end of the probe, changing the impedance. Instead of relying only on the conventional commercially available probes, the idea of designing a closed-ended coaxial

resonator by replacing the inner dielectric of the coaxial probe with the MUT is proposed in [36]. In both cases, the sample is in contact with the probe, which makes the probe susceptible to contamination and the measurements prone to error. To avoid any direct contact with the sample, cavities for contactless measurement have been introduced [37],[38]. In these cavities, a container is placed inside or close to the cavity, and the electric field is perturbed when the container is loaded with the sample. Figure 10 illustrates a cavity resonator with a container for contactless liquid characterization.

For instance, a cylindrical resonator for contactless measurement of NaCl solution (0%-5%) was proposed in [37]. This sensor includes a probe inserted into a cavity and a container to be filled with the saline solution. Among the main propagation modes (TE111, TM010, and TE011), the one with the highest quality factor and the largest separation from the other modes is chosen (TE011). Based on the perturbation theory, the variation in permittivity $\Delta\varepsilon$ is obtained.

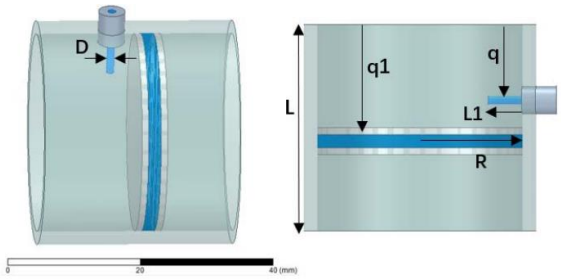

Figure 10. A cylindrical resonator with a container for loading the sample for contactless measurement of liquid concentration using dielectric spectroscopy [37].

3.2.2 Planar resonators

Despite having a higher quality factor, non-planar resonant sensors are often bulky, whereas in biomedical applications of dielectric spectroscopy, an appropriate platform for samples

with a volume as small as nL or µL is required. Although bulk sensors can be integrated with microfluidics [39], miniaturized planar sensors are more easily compatible with various microfluidic systems such as lab-on-a-chip, organ-on-a-chip, cell sorting and trapping, and flexible electronics and wearables.

In fact, basically any structure that forms an RLC circuit on a planar technology, such as CPW or microstrip, can be utilized as a planar resonant sensor; including but not limited to Split Ring Resonators (SRR), their dual counterparts Complementary Split Ring Resonators (CSRR), and interdigitated capacitors combined with other mentioned structures or solely with an inductance.

In this section, we will discuss how various microwave planar resonators have been introduced to the fields of chemistry and biology, focusing on more recent advances in applications of SRRs and CSRRs.

3.2.2.1 Split Ring Resonators

Planar split ring resonators make it possible to observe the occurrences close to the surface of a sensor, thanks to interaction of a biomatter with the highly concentrated electric field in the slit of a split ring. One newly developed example is a hairpin resonator for melanoma cell detection [40]. As the cell is trapped in a channel, the electromagnetic wave goes through the growth medium, enters the cells, and passes through the growth medium again to reach the other electrode. Although it is usually preferred to evaluate the change in transmission amplitude, the reflection (S_{11}) change is more pronounced than the transmission (S_{21}) change in this case. A higher variation in reflection due to the non-homogeneous interface between the cell and the medium explains this difference.

While trapping techniques often accommodate single-cell dielectric spectroscopy, Watts et al. [39] introduce a biosensor that consists of a double SRR that detects the free-flowing live cells moving in the microfluidic channel along the gap. This sensor cannot be considered entirely planar as it has a copper cavity for stimulation, and the gold ring resonator is deposited on a glass coverslip. Nevertheless, this hybrid configuration produces a large quality factor, even with lossy water.

Following the studies on dielectric spectroscopy for cells and bacteria [41],[42],[43], SRR-based sensors have been developed for real-time monitoring of bacteria concentration and growth [44],[45],[46] and the effect of glucose or antibiotics on this growth [47],[48]. As illustrated in Figure 11(a), the resonance frequency changes the most when the sample is placed over the ring gap, and so the bacteria growth medium is placed over the sensitive gap in SRR, and the corresponding capacitance and conductance gradually change over time, which is measured through the change in amplitude of the reflection or the transmission as well as the resonance frequency shift. The time-dependent variation of the resonance amplitude for two different volumes of E-coli (Figure 11 (b)) corresponds to the bacterial growth. As the simulation results in Figure 11 (c) and (d) confirm, the changes in the loss tangent contribute to changes in the amplitude, which can be translated into bacterial growth.

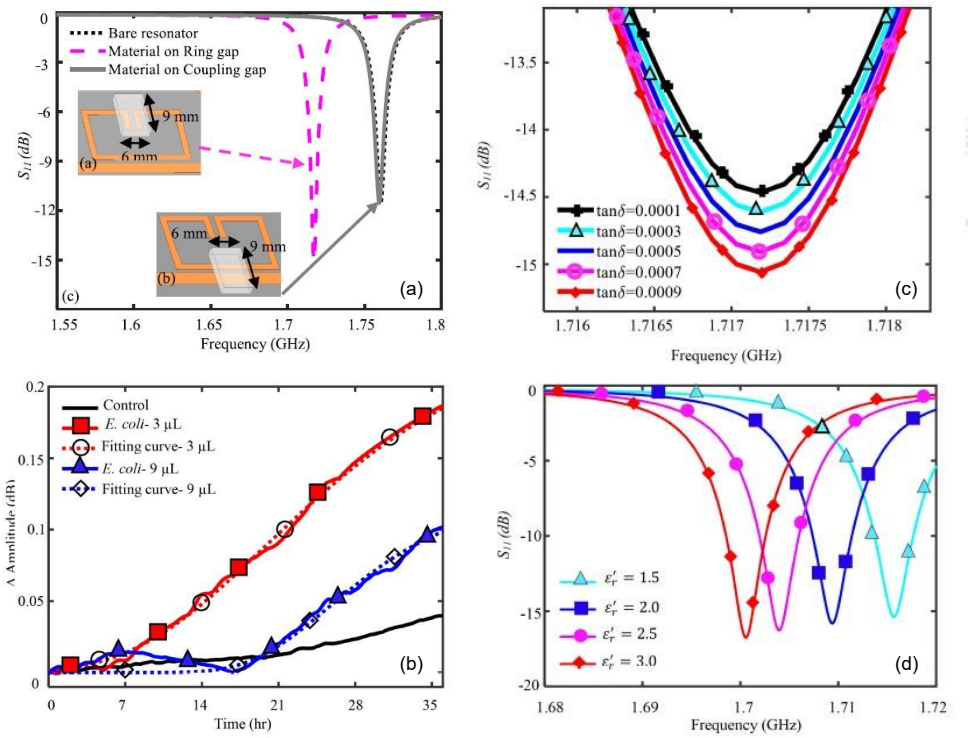

Figure 11. Planar Split Ring Resonator (SRR) sensor for bacterial growth monitoring in a real-time manner with (a) effect of putting the sample on the coupling gap or the ring gap, (b) shift in the amplitude of resonance during time due to bacterial growth and permittivity variation, and (c) and (d) simulation results that show resonance frequency and amplitude changes for different matter with different permittivity [44].

SRRs have also been implemented in tissue studies, focusing on the tissues' dielectric characteristics as a key feature of their physiological state. A microstrip ring resonator with CPW access (MRRC) has been devised to measure the dielectric parameters of animal tissues [49]. The sensor is made up of a microstrip ring resonator (MRR) on the top surface with CPW feed lines on the other side, and the sample is loaded as a superstrate on the MRR. The advantage of the proposed configuration compared to a simple MRR with a microstrip feedline is that the sample-induced losses do not affect the signal propagation in feedlines.

Same as the applications of Goubau line for broadband measurement of bio matter, at higher frequencies (~600 GHz), a THz-imaging technique based on SRR integrated with PGL is proposed in [50]. With a bare sensor resonance frequency of 596 GHz, healthy and cancerous colonic tissue models cause a 130 and 155 GHz frequency shift to lower frequencies, respectively. Nevertheless, the effective sensing depth of the sensor is limited to a few microns, limiting its performance in deeper analysis of a tissue.

3.2.2.2 Complementary Split Ring Resonators

CSRRs are one of the most popular planar resonators because of the strong electric field perpendicular to the CSRRs' surface, improving the penetration depth. This is important especially when a sample is not sensed in direct contact to the sensor as, for example, sensing the blood beneath multiple layers of skin or in a container to investigate blood glucose concentration or *in-vivo* tissue characterization. Omer et al. have developed several glucose sensors in a hexagonal CSRR form (honey cell) [51],[52],[53] and three circular CSRRs [54],[55] for wearable applications. An illustration is given in Figure 12. These studies not only present a novel structure compared to a single CSRR but also develop (1) a dipole antenna tag reader for distant sensing and (2) a radar-driven portable sensor to overcome the need for high-cost and bulky VNAs. The sensor's selectivity and specificity remain the main constraints in using dielectric spectroscopy for glycemia. The presence of other substances such as ions, proteins, and other molecules can negatively affect the repeatability and reproducibility of the measurements. However, the glucose concentration in the blood is dominant compared to these other components [51], enabling the design of microwave sensors for glycemia monitoring as a potential non-invasive replacement for currently available invasive and minimally-invasive solutions.

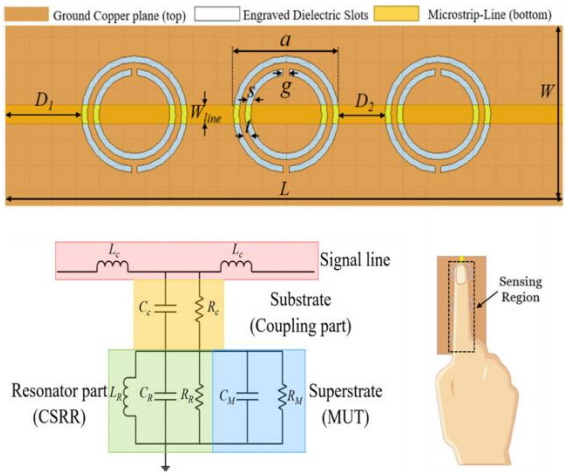

Figure 12. Triple CSRR sensor for non-invasive glucose measurement and equivalent electrical model of a single CSRR loaded with MUT [54].

Similar to the case of blood glucose biosensors, non-invasive in-vivo tissue spectroscopy requires a good penetration depth such that the signal passes through different layers. Furthermore, flexibility and spatial resolution are essential. For instance, Maenhout et al. [56] developed a flexible tubular device using CSRRs with high penetration depth to characterize colorectal tissue. The prototype is designed to be deployed in patients' colon and evaluate the tissue's health or malignancy in six directions (Figure 13).

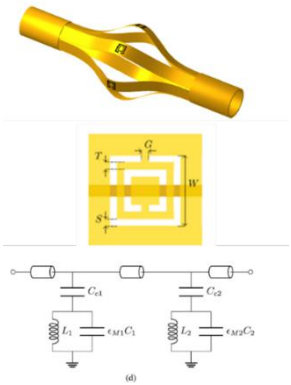

Figure 13. Flexible tubular device for colon tissue dielectric spectroscopy using three CSRRs and their equivalent electrical models [56].

Skin tissue and its abnormalities have also been considered a possible application of resonant microwave sensors [57] and CSRRs; as in [58], performance of a CSRR-based senor on a detection of cancerous cells in a skin tissue phantom is validated using simulations. Variation in the amplitude and phase of reflection and transmission coefficients in the frequency range of 2-18 GHz is correlated to the presence of cancer cells with higher water content in the epidermis of their developed skin model.

The resonant sensors and the characterized biological matter are not limited to what we discussed here; the research in this area is ongoing, aiming to improve the specifications such as quality factor and sensitivity, for a more precise detection.

4. Conclusions and Future Perspectives

In conclusion, the field of DS is large and growing. This non-ionizing, non-invasive and label-free characterization technique is already employed for biological matter in the detection of cancer biomarkers, glucose sensing in diabetes patients and many more areas, and can be adapted for the characterization of any type of biological matter on a continuously lowering scale as the operating frequencies rise through the development of new measurement technologies and equipment. The biomedical applications of dielectric spectroscopy are not limited to the ones mentioned here, neither are the technologies only valuable on their own. Combining different DS techniques as well as combining DS techniques with other characterization methods e.g., electrochemical analysis, can allow us to achieve measurements in a broader frequency range [59], [60]. Moreover, artificial intelligence has yet to improve this field as drastically as it did a lot of scientific domains in the last decades: Machine Learning algorithms can be applied in the design process [61], or in data analysis, such as for classification [62] or personalized sensor calibration, to improve the performance

of dielectric spectroscopy. Despite the advances in sensor miniaturization as well as measurement techniques and instruments, bringing dielectric spectroscopy to point-of-care applications remains challenging. Large, complicated, and costly VNA setups which require calibration before measurements restrain the application of the sensors for untrained users. Moreover, it causes the devices to be a chip-in-a-lab rather than a lab-on-a-chip. Recent progress in the development of VNA-on-a-chip is considered a game changer in that regard and is expected to bring the devices into the mobile testing domain. Finally, dielectric spectroscopy combined with microwave heating brings up new possibilities in cancer theranostics; the tumor can be detected through dielectric spectroscopy (diagnostics) and specifically targeted as its dielectric properties alter its sensitivity to ablation techniques (therapeutics).

References

[1] World Health Organization, “Cancer,” Who. https://www.who.int/news-room/factsheets/detail/cancer.

[2] Y. Pan et al., “3D cell-based biosensor for cell viability and drug assessment by 3D electric cell/matrigel-substrate impedance sensing,” *Biosens. Bioelectron.*, vol. 130, pp. 344–351, Apr. 2019, doi: 10.1016/j.bios.2018.09.046.

[3] M. A. Aldhaeebi, K. Alzoubi, T. S. Almoneef, S. M. Bamatraf, H. Attia, and O. M. Ramahi, “Review of microwaves techniques for breast cancer detection,” *Sensors*, vol. 20, no. 8, p. 2390, Apr. 2020, doi: 10.3390/s20082390.

[4] P. Mehrotra, B. Chatterjee, and S. Sen, “EM-wave biosensors: A review of RF, microwave, mm-wave and optical sensing,” *Sensors,* vol. 19, no. 5, p. 1013, Feb. 2019, doi: 10.3390/s19051013.

[5] H. P. Schwan, "Electrical Properties of Tissue and Cell Suspensions," *Advances in Biological and Medical Physics*, vol. 5, Elsevier, 1957, pp. 147-209.

[6] G. Maenhout, “Dielectric detection and ablation techniques for cancer theranostics,” PhD dissertation, KU Leuven, Leuven, 2022.

[7] J. C. M. Hwang, “Label-free noninvasive cell characterization: A methodology using broadband impedance spectroscopy,” *IEEE Microw. Mag.*, vol. 22, no. 5, pp. 78–87, May 2021, doi: 10.1109/MMM.2021.3056834.

[8] Keysight Technologies, “Basics of Measuring the Dielectric Properties of Materials,” *Keysight Technologies*, Aug. 2020.

[9] C. Aydinalp, S. Joof, I. Dilman, I. Akduman, and T. Yilmaz, “Characterization of open-ended coaxial probe sensing depth with respect to aperture size for dielectric property measurement of heterogeneous tissues,” *Sensors*, vol. 22, no. 3, p. 760, Jan. 2022, doi: 10.3390/s22030760.

[10] M. Lazebnik *et al.*, "A large-scale study of the ultrawideband microwave dielectric properties of normal, benign and malignant breast tissues obtained from cancer surgeries,", *Phys. Med. Biol,* vol. 52, no. 20, pp. 6093-115, Oct. 2007, doi: 10.1088/0031-9155/52/20/002.

[11] A. P. O'Rourke *et al.*, "Dielectric properties of human normal, malignant and cirrhotic liver tissue: in vivo and ex vivo measurements from 0.5 to 20 GHz using a precision open-ended coaxial probe," *Phys. Med. Biol,* vol. 52, no. 15, p. 4707, Jul. 2007, doi: 10.1088/0031-9155/52/15/022.

[12] T. Yilmaz *et al.*, "Microwave dielectric spectroscopy of renal calculi: A large scale study on dielectric properties from 500 MHz to 18 GHz," *IEEE Trans. Dielectrics Elect. Insul.,* vol. 26, no. 5, pp. 1425-1433, 2019, doi: 10.1109/TDEI.2019.008029.

[13] S. Liu *et al.*, "Hybrid characterization of nanolitre dielectric fluids in a single microfluidic channel up to 110 GHz," *IEEE Trans. Microw. Theory Techn.*, vol. 65, no. 12, pp. 5063–5073, Dec. 2017, doi: 10.1109/TMTT.2017.2731950.

[14] Rainee N. Simons, *Coplanar Waveguide Circuits, Components, and Systems*. John Wiley & Sons, 2001.

[15] Unknown Editor, "Coplanar Waveguide," Microwaves101. https://www.microwaves101.com/encyclopedias/coplanar-waveguide.

[16] F. Artis *et al.*, "Microwaving biological cells: Intracellular analysis with microwave dielectric spectroscopy," *IEEE Microw. Mag.*, vol. 16, no. 4, pp. 87–96, Mar. 2015, doi: 10.1109/MMM.2015.2393997.

[17] K. Grenier *et al.*, "Recent advances in microwave-based dielectric spectroscopy at the cellular level for cancer investigations," *IEEE Trans. Microw. Theory Techn.*, vol. 61, no. 5, pp. 2023–2030, Apr. 2013, doi: 10.1109/TMTT.2013.2255885.

[18] X. Du, C. Ferguson, X. Ma, X. Cheng, and J. C. M. Hwang, “Ultra-wideband impedance spectroscopy of the nucleus in a live cell,” *IEEE J. Electromagn. RF Microw. Med. Biol.*, vol. 6, no. 2, pp. 267–272, Jun. 2022, doi: 10.1109/JERM.2021.3121258.

[19] O. Peytral-Rieu, K. Grenier, and D. Dubuc, “Microwave sensor dedicated to the determination of the dielectric properties of 3D biological models from 500 MHz to 20 GHz,” in *2021 IEEE MTT-S Int. Microw. Symp. (IMS)*, Jun. 2021, pp. 222–225. doi: 10.1109/IMS19712.2021.9574794.

[20] A. Zedek, D. Dubuc, and K. Grenier, “Microwave permittivity extraction of individual biological cells submitted to different stimuli,” in *IEEE MTT-S Int. Microw. Symp. Dig.*, Jun. 2017, pp. 865–868 doi: 10.1109/MWSYM.2017.8058718.

[21] A. Tamra, M. P. Rols, D. Dubuc, and K. Grenier, “Impact of a chemical stimulus on two different cell lines through microwave dielectric spectroscopy at the single cell level,” in *Proc. IEEE MTT-S Int. Microw. Biom. Conf. (IMBioC)*, May 2019, pp. 1–4 doi: 10.1109/IMBIOC.2019.8777745.

[22] A. Tamra, A. Zedek, M.-P. Rols, D. Dubuc, and K. Grenier, “Single cell microwave biosensor for monitoring cellular response to electrochemotherapy,” *IEEE Trans. Biomed. Eng.*, pp. 1–1, Apr. 2022, doi: 10.1109/TBME.2022.3170267.

[23] F. Artis, D. Dubuc, J.-J. Fournie, M. Poupot, and K. Grenier, “Microwave dielectric spectroscopy of cell membrane permeabilization with saponin on human B lymphoma cells,” in *2014 IEEE MTT-S Int. Microw. Symp. (IMS),* Jun. 2014, pp. 1–4. doi: 10.1109/MWSYM.2014.6848520.

[24] A. Tamra, M. P. Rols, D. Dubuc, and K. Grenier, “Impact of a chemical stimulus on two different cell lines through microwave dielectric spectroscopy at the single cell level,” in *Proc. IEEE MTT-S Int. Microw. Biom. Conf. (IMBioC)*, May 2019, pp. 1–4 doi: 10.1109/IMBIOC.2019.8777745.

[25] A. Tamra, A. Zedek, M.-P. Rols, D. Dubuc, and K. Grenier, “Single cell microwave biosensor for monitoring cellular response to electrochemotherapy,” *IEEE Trans. Biomed. Eng.*, pp. 1–1, Apr. 2022, doi: 10.1109/TBME.2022.3170267.

[26] G. Poiroux *et al.*, “Label-free detection of mitochondrial activity with microwave dielectric spectroscopy,” *Int. J. Biotechnol. Bioeng.*, Jul. 2020.

[27] D. Dubuc, K. Grenier, F. Morfoisse, and B. Susini-Garmy, “In vitro and in vivo investigations toward near-field microwave-based detection of melanoma,” in *2017 IEEE MTT-S Int. Microw. Biom. Conf. (IMBioC)*, May 2017, pp. 1–4. doi: 10.1109/IMBIOC.2017.7965789.

[28] O. Peytral-Rieu, D. Dubuc, and K. Grenier, "Microwave Microfabricated Sensor Dedicated to the Dielectric Characterization of Biological Microtissues," in *2022 URSI Atlantic and Asia Pacific Radio Science Meeting (AT-AP-RASC)*, Jun. 2022, pp. 1-4, doi: 10.23919/AT-AP-RASC54737.2022.9814189.

[29] T. Chen, F. Artis, D. Dubuc, J.-J. Fournie, M. Poupot, and K. Grenier, “Microwave biosensor dedicated to the dielectric spectroscopy of a single alive biological cell in its culture medium,” in *IEEE MTT-S Int. Microw. Symp. Dig.*, Jun. 2013, pp. 1–4. doi: 10.1109/MWSYM.2013.6697740.

[30] S. Nourinovin, M. M. Rahman, R. C. Jones, M. P. Philpott, and A. Alomainy, "Impact of Drug Treatment on the Electromagnetic Properties of Basal Cell Carcinoma Cancer in the Terahertz Band," *in 2022 Eur. Conf. Antennas Propag. (EuCAP)*, Apr. 2022, pp. 1-4, doi: 10.23919/EuCAP53622.2022.9769353.

[31] X. Wu *et al*., "Biomedical applications of terahertz spectra in clinical and molecular pathology of human glioma," *Spectrochim. Acta A: Mol. Biomol. Spectrosc.*, vol. 285, 2023, doi: 10.1016/j.saa.2022.121933.

[32] P. Yu *et al*., "Myocardial Amyloidosis Detection with Terahertz Spectroscopy," *IEEE Sensors J.*, vol. 22, no. 3, pp. 2389-2398, Feb. 2022, doi: 10.1109/jsen.2021.3133294

[33] I. Nardecchia *et al*., "Out-of-Equilibrium Collective Oscillation as Phonon Condensation in a Model Protein," *Physical Rev. X*, vol. 8, no. 3, p. 031061, Oct. 2018, doi: 10.1103/PhysRevX.8.031061.

[34] M. Lechelon *et al*., "Experimental evidence for long-distance electrodynamic intermolecular forces," *Sci. Advances*, vol. 8, no. 7, Feb. 2022, doi: 10.1126/sciadv.abl5855.

[35] S. Laurette, A. Treizebre, and B. Bocquet, "Co-integrated microfluidic and THz functions for biochip devices," *J. Micromechanics and Microengineering,* vol. 21, no. 6, p. 065029, May 2011, doi: 10.1088/0960-1317/21/6/065029.

[36] A. M. Mohammed, Y. Wang, and M. J. Lancaster, "3D printed coaxial microwave resonator sensor for dielectric measurements of liquid," *Microw. Opt. Technol. Lett.*, vol. 63, no. 3, pp. 805–810, Mar. 2021, doi: 10.1002/mop.32679.

[37] Y. J. Mao, Y. J. Zhang, Z. R. Chen, and M. S. Tong, "A noncontact microwave sensor based on cylindrical resonator for detecting concentration of liquid solutions," *IEEE Sensor J.*, vol. 21, no. 2, pp. 1208–1214, Jan. 2021, doi: 10.1109/JSEN.2020.3016290.

[38] R. S. Hassan, S. I. Park, A. K. Arya, and S. Kim, "Continuous characterization of permittivity over a wide bandwidth using a cavity resonator," *J. Electromagn. Eng. Sci.*, vol. 20, no. 1, pp. 39–44, Jan. 2020, doi: 10.26866/jees.2020.20.1.39.

[39] C. Watts, S. M. Hanham, J. P. K. Armstrong, M. M. Ahmad, M. M. Stevens, and N. Klein, "Microwave dielectric sensing of free-flowing, single, living cells in aqueous suspension," *IEEE J. Electromagn. RF Microw. Med. Biol.*, vol. 4, no. 2, pp. 97–108, Jun. 2020, doi: 10.1109/JERM.2019.2932569.

[40] C. F. Liu, M. H. Wang, and L. S. Jang, "Microfluidics-based hairpin resonator biosensor for biological cell detection," *Sens. Actuators B, Chem.*, vol. 263, pp. 129–136, Jun. 2018, doi: 10.1016/j.snb.2018.01.234.

[41] I. Piekarz *et al.*, "Planar single and dual-resonant microwave biosensors for label-free bacteria detection," *Sens. Actuators B, Chem.*, vol. 351, Jan. 2022, doi: 10.1016/j.snb.2021.130899.

[42] M. Russel *et al.*, "High-frequency, dielectric spectroscopy for the detection of electrophysiological/biophysical differences in different bacteria types and concentrations," *Anal. Chim. Acta*, vol. 1028, pp. 86–95, Oct. 2018, doi: 10.1016/j.aca.2018.04.045.

[43] G. Bridges, T. Cabel, S. Afshar, E. Salimi, D. Thomson, and M. Butler, "Microwave near-field detection of single biological cells and nanoparticles," in *2018 Int. Symp. Antenna Technol. Appl. Electromagn. (ANTEM)*, Aug. 2018, pp. 1–2. doi: 10.1109/ANTEM.2018.8572975.

[44] M. C. Jain, A. V. Nadaraja, S. Mohammadi, B. M. Vizcaino, and M. H. Zarifi, "Passive microwave biosensor for real-time monitoring of subsurface bacterial growth," *IEEE Trans. Biomed. Circuits Syst.*, vol. 15, no. 1, pp. 122–132, Feb. 2021, doi: 10.1109/TBCAS.2021.3055227.

[45] R. Narang *et al.*, "Sensitive, real-time and non-intrusive detection of concentration and growth of pathogenic bacteria using microfluidic-microwave ring resonator biosensor," *Sci. Rep.*, vol. 8, no. 1, Dec. 2018, doi: 10.1038/s41598-018-34001-w.

[46] S. Mohammadi, R. Narang, M. Mohammadi Ashani, H. Sadabadi, A. Sanati-Nezhad, and M. H. Zarifi, "Real-time monitoring of Escherichia coli concentration with planar microwave

resonator sensor," *Microw. Opt. Technol. Lett.*, vol. 61, no. 11, pp. 2534–2539, Nov. 2019, doi: 10.1002/mop.31913.

[47] M. C. Jain, A. V. Nadaraja, B. M. Vizcaino, D. J. Roberts, and M. H. Zarifi, "Differential microwave resonator sensor reveals glucose-dependent growth profile of E. coli on solid agar," *IEEE Microw. Wireless Compon. Lett.*, vol. 30, no. 5, pp. 531–534, May 2020, doi: 10.1109/LMWC.2020.2980756.

[48] M. C. Jain, A. V. Nadaraja, R. Narang, and M. H. Zarifi, "Rapid and real-time monitoring of bacterial growth against antibiotics in solid growth medium using a contactless planar microwave resonator sensor," *Sci. Rep.*, vol. 11, no. 1, Dec. 2021, doi: 10.1038/s41598-021-94139-y.

[49] F. Deshours *et al.*, "Improved microwave biosensor for non-invasive dielectric characterization of biological tissues," *Microelectronics J.*, vol. 88, pp. 137–144, Jun. 2019, doi: 10.1016/j.mejo.2018.01.027.

[50] S. J. Park, R. Tucker, E. Pickwell-MacPherson, and J. E. Cunningham, "Design of a split ring resonator integrated with on-chip terahertz waveguides for colon cancer detection," *Adv. Theory Simul.*, p. 2200313, Jul. 2022, doi: 10.1002/adts.202200313.

[51] A. E. Omer *et al.*, "Low-cost portable microwave sensor for non-invasive monitoring of blood glucose level: novel design utilizing a four-cell CSRR hexagonal configuration," *Sci. Rep.*, vol. 10, no. 1, Dec. 2020, doi: 10.1038/s41598-020-72114-3.

[52] A. E. Omer, G. Shaker, and S. Safavi-Naeini, "Portable radar-driven microwave sensor for intermittent glucose levels monitoring," *IEEE Sens. Lett.*, vol. 4, no. 5, May 2020, doi: 10.1109/LSENS.2020.2986208.

[53] A. E. Omer, G. Shaker, S. Safavi-Naeini, H. Kokabi, G. Alquie, and F. Deshours, “Compact honey-cell CSRR-based microwave newline biosensor for monitoring glucose levels,” in *2020 Eur. Conf. Antennas Propag. (EuCAP)*, Mar. 2020, pp. 1–5. doi: 10.23919/EuCAP48036.2020.9135301.

[54] A. E. Omer *et al.*, “Non-invasive real-time monitoring of glucose level using novel microwave biosensor based on triple-pole CSRR,” *IEEE Trans. Biomed. Circuits Syst.*, Nov. 2020, doi: 10.1109/TBCAS.2020.3038589.

[55] A. E. Omer, G. Shaker, and S. Safavi-Naeini, “Wearable CSRR-based sensor for monitoring glycemic levels for diabetics,” in *Proc. IEEE 20th Int. Conf. Bioinf. Bioeng.*, Oct. 2020, pp. 922–928. doi: 10.1109/BIBE50027.2020.00156.

[56] G. Maenhout, T. Markovic, and B. Nauwelaers, “Flexible, segmented tubular design with embedded complementary split-ring resonators for tissue identification,” *IEEE Sensors J.*, vol. 21, no. 14, pp. 16024–16032, Jul. 2021, doi: 10.1109/JSEN.2021.3075570.

[57] J. Bai, H. Guo, H. Li, C. Zhou, and H. Tang, “Flexible microwave biosensor for skin abnormality detection based on spoof surface plasmon polaritons,” *Micromachines*, vol. 12, no. 12, Dec. 2021, doi: 10.3390/mi12121550.

[58] M. K. Sharma, R. Kumari, A. Mittal, M. K. Upadhyay, A. Mittal, and K. Singh, "Design and Modeling of the Ring Resonator-Based Microwave Sensor for Skin Cancer Detection," in *Flexible Electronics for Electric Vehicles*, 2023: Springer Nature Singapore, pp. 47-58.

[59] X. Bao *et al.*, “Broadband dielectric spectroscopy of cell cultures,” *IEEE Trans. Microw. Theory Techn.*, vol. 66, no. 12, pp. 5750–5759, Dec. 2018, doi: 10.1109/TMTT.2018.2873395.

[60] G. M. Dittami, H. E. Ayliffe, C. S. King, and R. D. Rabbitt, “A multilayer MEMS platform for single-cell electric impedance spectroscopy and electrochemical analysis,” *J. Microelectromech. Syst.*, vol. 17, no. 4, pp. 850–862, Aug. 2008, doi: 10.1109/JMEMS.2008.921726.

[61] B. X. Wang, W. S. Zhao, D. W. Wang, J. Wang, W. Li, and J. Liu, “Optimal design of planar microwave microfluidic sensors based on deep reinforcement learning,” *IEEE Sensors J.*, vol. 21, no. 24, pp. 27441–27449, Dec. 2021, doi: 10.1109/JSEN.2021.3124294.

[62] J. A. Osterberg *et al.*, “Microwave sensing of yeast cell species and viability,” *IEEE Trans. Microw. Theory Techn.*, vol. 69, no. 3, pp. 1875–1886, Mar. 2021, doi: 10.1109/TMTT.2020.3048176.